Engineering Journal of University of Qatar, Vol. 9, 1996, p.123 - 132

IMPROVED 3D-FE COMPUTATIONAL METHOD FOR MAGNETOSTATIC FIELD PROBLEMS USING UNCONSTRAINED VECTOR POTENTIAL

Mohamed A. Alhamadi
Department of Electrical Engineering
University of Qatar, Doha, Qatar.

ABSTRACT

This paper introduces an improved three dimensional finite-element (3D-FE) computational approach for magnetostatic field problems using unconstrained magnetic vector potential (MVP) formulation in conjunction with hexahedral type elements. It was found that the use of first order or second order hexahedral type element in the FE formulation eliminates the sensitivity of the FE computational results to grid geometries and elemental shape ill-conditioning associated with first order tetrahedral type elements. The method is shown to be computationally economical and is highly recommended for large scale global type 3D magnetostatic field computations in electrical devices.

INTRODUCTION

A review of literature reveals that the use of vector potential formulation for the computation of three dimensional (3D) magnetostatic fields by finite elements (FE) have been associated with the enforcement of the divergence of the MVP, $\overline{A}$, to zero (1,2). Such constraint was applied due to concerns about the impact of the unconstrained $(\nabla \cdot \overline{A})$ on the uniqueness of the computed values of the MVP. Later investigations concluded that under usual conditions assumed in a 3D-FE computation, it is not necessary to specify $\nabla \cdot \overline{A}$ in order to uniquely define the vector potential $\overline{A}$ (3).

Wang and Demerdash (4) found that the first order FE method works quite well in conjunction with the unconstrained MVP formulations in the computations of 3D magnetostatic fields in single medium applications. Yet the method failed to give satisfactory results in the mixed-media (air-iron) applications because of the substantial sensitivity of the results to grid geometries and consequent elemental shape ill-conditioning. Such unconstrained

MVP formulation was based on the first order tetrahedral finite elements. In addition, the authors found that the use of higher order, such as second order, tetrahedral elements yields results which are almost insensitive to grid geometries and associated elemental shape ill-conditioning.

In this work, the effort was made to evaluate the element properties based on elemental shape function specifications and on the order of integration (5). It is demonstrated here that the use of the unconstrained MVP formulation in conjunction with either first or higher order hexahedral FE appears to thoroughly alleviate sensitivities of the computational results to grid geometries and possible effects of numerical ill-conditioning. Although a hexahedron has more complex types of shape functions than a simple tetrahedron, it is demonstrated that the use of hexahedral elements in the FE formulation reduces the very large numbers of simultaneous equations generated by the tetrahedral based FE formulation. Accordingly, this approach possesses substantial savings in the computer CPU time and storage over a second order tetrahedral FE approach. The method was applied to a demonstration example, namely a 1.5 kVA shell-type laminated iron core transformer, the geometry of which is given in Figure (1).

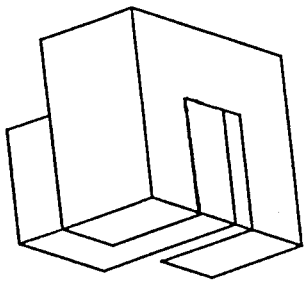

Fig. 1. One octant of a 1.5 kVA transformer

THE UNCONSTRAINED MVP METHOD

The MVP-FE formulation is based on the solution of the curl-curl partial differential equation which governs the MVP, $\bar{A}$,or a given set of boundary conditions. That is,

$$\nabla \times (\bar{\bar{\upsilon}} \cdot \nabla \times \bar{A}) = \bar{J} \qquad (1)$$

where $\overline{\overline{\upsilon}}$ is the tensor of anisotropic reluctivity of the medium, and $\bar{J}$ is the distributed source current density vector.

The corresponding energy functional to be minimized in the FE formulation is as follows (6):

$$F(\bar{A})=\int_V\left[\frac{1}{2}(\bar{B}\cdot\bar{H})-\bar{J}\cdot\bar{A}\right]dv \tag{2}$$

where V is the global solution volume.

In order to minimize the functional of equation (2), the associated solution region is subdivided into hexahedral elements. Hence, equation (2) can be expressed by a summation of volume integrations in every element as follows:

$$F=\sum_{e=1}^{NE}F_e=\sum_{e=1}^{NE}\int_{Ve}\left[\frac{1}{2}(\bar{B}\cdot\bar{H})-\bar{J}\cdot\bar{A}\right]dv \tag{3}$$

where NE is the total number of elements in a given FE grid. The functional $F(\bar{A})$ is minimized by setting its derivatives with respect to the three directional components of MVP at each node to zero. That is:

$$\frac{\partial F}{\partial A_{ix}}=0,\ \frac{\partial F}{\partial A_{iy}}=0,\ \frac{\partial F}{\partial A_{iz}}=0,\ \text{for } i=1,2,\ldots,NN \tag{4}$$

where NN is the total number of elements in a given FE grid. These differential equations are taken for every hexahedral element and yield a set of elemental equations. This paper next introduces the elemental equations based on a first order hexahedron and on a second order hexahedron as basic building blocks in the FE grid descritization.

The Hexahedral Finite Element Formulation:

The magnetic vector potential, $\bar{A}$, within an element can be expressed by the following interpolation polynomial:

$$\bar{A}=\sum_{k=1}^{nn}N_k\bar{A}_k=\sum_{k=1}^{nn}N_k(A_{kx}\hat{a}_x+A_{ky}\hat{a}_y+A_{kz}\hat{a}_z) \tag{5}$$

where, nn is the number of nodes in a hexahedral element, and is equal to 8 for a first order element or equal to 20 for a second order element, whereas N_k is the shape function associated with the k-th node of the element, and $\overline{A}_k$ is the nodal vector potential at the k-th node. The element equations can be written in a general matrix form as follows:

$$\underline{S}_e \cdot \underline{A}_e = \underline{I}_e \tag{6}$$

where, $\underline{S}_e$ is the elemental stiffness matrix with a size of (3nn × 3nn) and can be defined for the ik-th entry as follows:

$$\underline{S}_{ik} = \left[\begin{array}{c|c|c} \int_{v_e} \nu_y \frac{\partial N_i}{\partial z}\frac{\partial N_k}{\partial z} dv + \int_{v_e} \nu_z \frac{\partial N_i}{\partial y}\frac{\partial N_k}{\partial y} dv & -\int_{v_e} \nu_z \frac{\partial N_i}{\partial y}\frac{\partial N_k}{\partial x} dv & -\int_{v_e} \nu_y \frac{\partial N_i}{\partial z}\frac{\partial N_k}{\partial x} dv \\ \hline -\int_{v_e} \nu_z \frac{\partial N_i}{\partial x}\frac{\partial N_k}{\partial y} dv & \int_{v_e} \nu_x \frac{\partial N_i}{\partial z}\frac{\partial N_k}{\partial z} dv + \int_{v_e} \nu_z \frac{\partial N_i}{\partial x}\frac{\partial N_k}{\partial x} dv & -\int_{v_e} \nu_x \frac{\partial N_i}{\partial z}\frac{\partial N_k}{\partial y} dv \\ \hline -\int_{v_e} \nu_y \frac{\partial N_i}{\partial x}\frac{\partial N_k}{\partial z} dv & -\int_{v_e} \nu_x \frac{\partial N_i}{\partial y}\frac{\partial N_k}{\partial z} dv & \int_{v_e} \nu_y \frac{\partial N_i}{\partial x}\frac{\partial N_k}{\partial x} dv + \int_{v_e} \nu_x \frac{\partial N_i}{\partial y}\frac{\partial N_k}{\partial y} dv \end{array}\right] \tag{7}$$

Meanwhile, $\underline{A}_e$ is a column vector which contains the unknown nodal components of the elemental MVPs with a size of (3nn × 1). The i-th entry of this column vector is given by:

$$\underline{A}_i = \left[A_{ix}\ A_{iy}\ A_{iz}\right]^T \tag{8}$$

Also, $\underline{I}_e$ is the elemental forcing function column vector with a size of (3nn × 1). The i-th entry of this column vector is defined by:

$$\underline{I}_i = \left[\int_{v_e} N_i J_x dv \int_{v_e} N_i J_y dv \int_{v_e} N_i J_z dv\right]^T \tag{9}$$

The various terms in equations (7) and (9) are discussed further in the appendix.

APPLICATION EXAMPLE AND RESULTS

The 3D-FE method based on the unconstrained MVP formulation was used in the magnetic field computation of one octant of a 1.5 kVA shell-type transformer, Figure (1). The field was computed at low excitation current of 0.25A to ensure no saturation in the laminated core. This was done in order to avoid the effect of saturation on the results of various solution methods in the comparison at hand. The 3D field computation was carried out using first order hexahedral FE. Two corresponding FE grids are shown in Figure (2). Notice that the two nodes A and B and their associated grid lines are shifted in grid #1 from their correspondings in grid #2. The computational results of the associated stored energy and magnetizing inductance are given in Table (1). Notice that the magnetizing inductance values obtained for the two FE grids reveal stable and insignificant change in the solution with respect to the change in the FE grid. The results of this approach were compared with computational results based on first order tetrahedral FE grid discretization for both grids #1 and #2, see Table (1). Comparison between the two approaches reveals that the hexahedral based FE solutions are less sensitive to grid changes and the computed magnetizing inductance is much closer to the measured value than the corresponding solutions obtained from the tetrahedral based FE. Furthermore, Figure (3) demonstrates the advantage of using first order hexahedral based FE over the use of first order tetrahedral based FE by comparing the adequate number of nodal equations required by each approach to achieve the desired accuracy of the results.

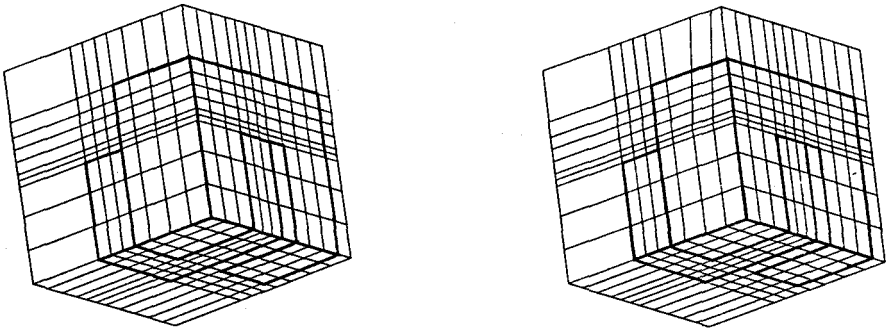

Grid #1 Grid #2

Fig. 2. First order hexahedral FE grids

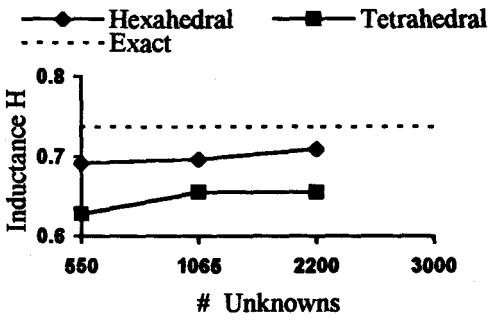

Fig. 3. Comparison on accuracy of 1st order results

Table 1. First Order 3D-FE Results (I = 0.25 A)

Grid	Type of Element	# Elements	# Un-knowns	Energy mJ	Inductance H
#1	Hexa.	880	2200	2.7581	0.709433
#2	Hexa.	880	2200	2.7527	0.711098
#1	Tetra.	5280	2200	2.5689	0.655471
#2	Tetra.	5280	2200	2.5661	0.662821
Measured Value of Inductance: 0.737 H					

Next, the 3D field computation was carried out using second order hexahedral FE for two grid discretizations, Figure (4). The results of this approach were compared with computational results based on corresponding second order tetrahedral FE grid discretizations, see Table (2). The effect of grid alteration on the sensitivity of the computed results in both approaches is insignificant. Also, the magnetizing inductance values calculated in both approaches are very close to the measured value. However, one may notice the substantial reduction in the computer storage and CPU time by the hexahedral based FE method. Such savings in the computer storage and CPU time could be immense in large-scale magnetostatic field computations with the involvement of iterative process due to nonlinear magnetic saturation.

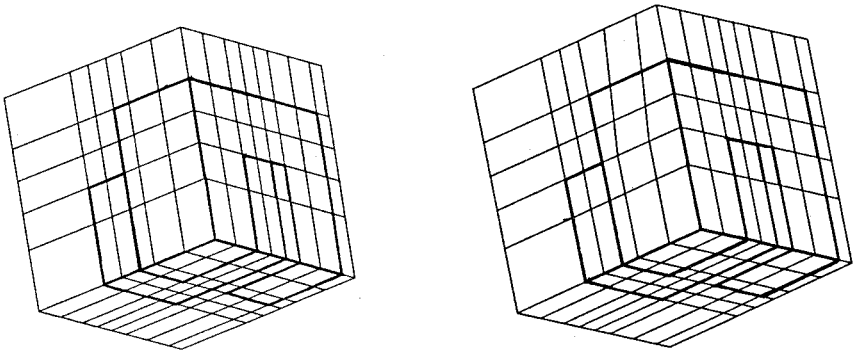

Grid #1 Grid #2

Fig. 4. Second order hexahedral FE grids

Table 2. Second Order 3D-FE Results (I = 0.25 A)

Grid	Type of Element	# Elements	# Unknowns	Energy mJ	Inductance H	CPU Time min.
#1	Hexa.	336	3341	2.9052	0.740933	89
#2	Hexa.	336	3341	2.8912	0.740504	81
#1	Tetra.	1440	5045	2.8604	0.727081	108
#2	Tetra.	1440	5045	2.8565	0.725173	110
Measured Value of Inductance: 0.737 H						

CONCLUSIONS

An improved 3D-FE computational approach for magnetostatic field problems using unconstrained MVP formulation in conjunction with hexahedral type elements has been presented. It was found that the use of first or second order hexahedral elements in the FE formulation yields stable and insensitive results to grid geometries and elemental shape ill-conditioning associated with first order tetrahedral elements. The method is also computationally economical in comparison to unconstrained MVP method with higher order tetrahedral type FE which may place severe limitations on the use of the method in practice. This is due to the excessive number of elemental equations to be used to achieve a given

degree of accuracy. In addition, the division of a space volume into individual tetrahedra presents difficulties of visualization and could easily lead to errors in nodal connections.

REFERENCES

1. **Coulomb, J.L., 1981.** "Finite Element Three Dimensional Magnetic Field Computation," *IEEE Trans. on MAG*, Vol. 17, p. 3241.

2. **Chari, M.V.K., Silvester, P.P., Konrad, A. and Palmo, M.A., 1981.** "Three-Dimensional Magnetostatic Field Analysis of Electrical Machinery by the Finite Element Method," *IEEE Trans. on PAS*, Vol. 100, p. 4007.

3. **Demerdash, N.A. and Wang, R., 1990.** "Theoretical and Numerical Difficulties in 3-D Vector Potential Methods in Finite Element Magnetostatic Computations," *IEEE Trans. on MAG*, Vol. 26, p. 1656.

4. **Wang, R., and Demerdash, N.A., 1990.** "On the effects of Grid Ill-conditioning in Three Dimensional Finite Element Vector Potential Magnetostatic Field Computations," *IEEE Trans. on MAG*, Vol. 26, p. 2190.

5. **Zienkiewicz, O.C. and Taylor, R.L., 1989.** *The Finite Element Method*, Fourth Edition, McGraw-Hill (UK).

6. **Demerdash, N.A., Nehl, T.W. and Fouad, F.A., 1980.** "Finite Element Formulation and Analysis of Three Dimensional Magnetic Field Problems," *IEEE Trans. on MAG*, Vol. 16, p. 1092.

7. **Tong, P. and Rossettos, J.N., 1982.** *Finite Element Method - Basic Technique and Implementation*, Third Edition, MIT Press.

APPENDIX

Interpolation functions of first order hexahedron (7):

$$u=\sum_{k=1}^{8} N_k(\alpha,\beta,\gamma)u_k \tag{10}$$

in which,

$$N_k(\alpha,\beta,\gamma)=1/8(1+\alpha\alpha_k)(1+\beta\beta_k)(1+\gamma\gamma_k) \tag{11}$$

where α, β, γ are local coordinates of a right hexahedron.

Interpolation functions of second order hexahedron:

$$u=\sum_{k=1}^{20} N_k(\alpha,\beta,\gamma)u_k \tag{12}$$

in which,

$$\begin{aligned}
N_k(\alpha,\beta,\gamma)&=1/8(1+\alpha\alpha_k)(1+\beta\beta_k)(1+\gamma\gamma_k)\\
&\quad\times(\alpha\alpha_k+\beta\beta_k+\gamma\gamma_k-2) && k=1,\ldots,8\\
N_k(\alpha,\beta,\gamma)&=1/4(1-\alpha^2)(1+\beta\beta_k)(1+\gamma\gamma_k) && k=9,11,17,19\\
N_k(\alpha,\beta,\gamma)&=1/4(1-\beta^2)(1+\alpha\alpha_k)(1+\gamma\gamma_k) && k=10,12,18,20\\
N_k(\alpha,\beta,\gamma)&=1/4(1-\gamma^2)(1+\alpha\alpha_k)(1+\beta\beta_k) && k=13,14,15,16
\end{aligned} \tag{13}$$

Coordinate transformation and numerical integration:

The numerical integrations in equations (7) and (9) can be expressed in the local coordinates, and can be numerically solved using a third order Gaussian quadrature algorithm as follows:

$$\begin{aligned}
\iiint G\left(N_i,\frac{\partial N_j}{\partial x},\frac{\partial N_k}{\partial y},\frac{\partial N_l}{\partial z}\right)dv&=\int_{-1}^{1}\int_{-1}^{1}\int_{-1}^{1} G^*(\alpha,\beta,\gamma)\,d\alpha\,d\beta\,d\gamma\\
&=\sum_{i=1}^{3}\sum_{j=1}^{3}\sum_{k=1}^{3} W_iW_jW_kG^*(\alpha_i,\beta_j,\gamma_k)
\end{aligned} \tag{14}$$

where W_i, W_j, W_k are the weighting factors and α_i, β_j, γ_k are the stations of the third order Gaussian quadrature

j, k, l	W_i, W_j, W_k	α_i, β_j, γ_k
1	5/9	$-\sqrt{15}/5$
2	8/9	0
3	5/9	$\sqrt{15}/5$